Motional binding in InAs with a realistic surface potential

J. Slinkman
IBM General Technology Division, Essex Junction, Vermont 05452

An-zhen Zhang and R. E. Doezema
Department of Physics and Astronomy, University of Oklahoma, Norman, Oklahoma 73019
(Received 6 June 1988)

The spatial dependence of the effective mass occurring in mass-mismatched quantum wells leads to a dependence of binding energy on transverse momentum. This "motional binding" has been observed in accumulation layers on narrow-band-gap materials, where the nonparabolicity provides the spatial dependence of the effective mass. To date, however, only a qualitative comparison has been made between experiment and theory. Here we use a model surface potential and a self-consistent potential to study motional binding in n-type InAs accumulation layers and find good agreement with experiment. The calculation shows that subbands are occupied over considerably larger ranges of surface-electron concentration than previously thought.

I. INTRODUCTION

Recently it was pointed out[1] that quantum wells with mass-mismatched barriers possess subbands with unusual dispersion properties for motion transverse to the confinement direction. Depending on the sign of the mass mismatch, either carrier binding or debinding can occur at a particular value k_c of the transverse wave vector k_t. For "motional binding," where a carrier is bound only for $k_t > k_c$, it was found that accumulation layers on degenerate, narrow-gap semiconductors provide an excellent example. With a simple square-well model, it was shown that the observed[2-4] "pinning" of the Shubnikov–de Haas (SdH) frequency B_f, at total carrier density values N_s below that expected for the threshold occupancy, could qualitatively be explained by motional binding. In this paper, we show that the experimental results for accumulation layers on n-type InAs cited previously[2] as well as newer results for more heavily degenerate n-type InAs,[5] can be understood using the motional binding picture with more realistic surface potentials—an exponentially screened potential and a self-consistent potential.

II. THEORETICAL BACKGROUND

Our purpose in this paper is to investigate the motional binding phenomenon beyond the simple square-well approximation of Ref. 1. We present this study in two steps. First we use the two-band model to examine motional binding with a non-self-consistent, exponential potential function. Then, we examine motional binding with a self-consistent potential in the semiclassical approximation. We expect that, particularly for accumulation layers on degenerate semiconductors as discussed by Baraff and Appelbaum,[6] self-consistency is necessary to properly take account of the interplay between bound and extended states and their response to external fields.

A. Two-band model with exponential potential

We use the effective mass $\vec{\mathbf{k}}\cdot\vec{\mathbf{p}}$ method in the two-band approximation, i.e., where only the light-mass bands pertain and thus the free-electron kinetic energy terms can be neglected, where electron energies and wave functions are described by the matrix equation

$$\begin{bmatrix} \left[\frac{E_g}{2}-E+V(z)\right]\mathbf{I} & i\mathbf{P}\cdot\vec{\gamma} \\ -i\vec{\mathbf{P}}\cdot\vec{\gamma} & \left[-\frac{E_g}{2}-E+V(z)\right]\mathbf{I} \end{bmatrix} \begin{bmatrix} \mathbf{\Phi} \\ \mathbf{X} \end{bmatrix} = 0 \tag{1}$$

in formal analogy to the Dirac equation.[7] The gap energy is denoted by E_g and the momentum operator by $\vec{\mathbf{P}}$. The vector $\gamma = W_x\sigma_x\hat{\mathbf{x}} + W_y\sigma_y\hat{\mathbf{y}} + W_z\sigma_z\hat{\mathbf{z}}$ is defined in terms of the Pauli spin matrices σ_i and the matrix elements W_i of the velocity operator. $\mathbf{\Phi}$ and $\mathbf{X}$ are the (spinor) envelope functions for the conduction band and valence band, respectively. The 2×2 unit matrix is $\mathbf{I}$. We consider an ideal sample which occupies the infinite half-space $z>0$ with surface potential $V(z)$.

We assume ellipsoidal, constant-energy surfaces in the sample with rotation axis along the surface normal. The wave functions are then separable:

$$\begin{bmatrix} \vec{\mathbf{\Phi}}(\vec{\mathbf{r}}) \\ \mathbf{X}(\mathbf{r}) \end{bmatrix} = \begin{bmatrix} \mathbf{\Phi}(z) \\ \mathbf{X}(z) \end{bmatrix} e^{i\mathbf{k}_t\cdot\mathbf{r}}, \tag{2}$$

where $\vec{\mathbf{k}}_t = k_x\hat{\mathbf{x}} + k_x\hat{\mathbf{y}}$ is the transverse wave vector. With the condition that $\mathbf{\Phi}(z)$ and $\mathbf{X}(z)$ vanish at $z=0$ and $z=\infty$, the bound-state energies $E_j(k_t)$ can be found from Eq. (1) by eliminating $\mathbf{X}(z)$ and diagonalizing the resulting 2×2 matrix equation for $\mathbf{\Phi}(z)$. The result is given by

$$\left\{E_j^- - \frac{\beta_t k_t^2}{E_j^+} \mp (\beta_l \beta_t)^{1/2} k_t \left[\frac{dV}{dz}\right] \Big/ (E_j^+)^2 + \left[\beta_l \left[\frac{dV}{dz}\right] \Big/ (E_j^+)^2\right] \frac{d}{dz} + (\beta_l / E_j^+) \frac{d^2}{dz^2}\right\} \phi_\pm(z) = 0 \ , \tag{3}$$

where $E_j^\pm = E_j - V(z) \pm E_g/2$, and

$$\Phi(z) = \begin{bmatrix} 1 \\ \pm i k_t / k_- \end{bmatrix} \phi_\pm(z) \ ,$$

with $k_\pm = k_x \pm i k_y$.

The coefficients $\beta_{l,t}$ are given by $\hbar^2 E_g / 2 m_{l,t}^*$, where m_l^* and m_t^* are the longitudinal and transverse effective-mass components. These coefficients are related to the velocity matrix elements by $\beta_l = \hbar^2 W_z^2$ and $\beta_t = \hbar^2 (W_x^2 + W_y^2)$. Expressions similar to Eq. (3) have been given by Ohkawa and Uemura,[8,9] by Reisinger,[10] and by Takada *et al.*[11]

We solve Eq. (3) numerically for $V(z) = -V_0 e^{-z/\lambda}$. The parameters V_0 and λ are chosen appropriately for the InAs data; we also take $m_l^* = m_t^* = 0.023 m_0$ (free-electron mass) and $E_g = 410$ meV. For arbitrary values of the energy E_j and k_t, the solution of Eq. (3) was found by using a fourth-order Runge-Kutta method to integrate the wave function $\phi_\pm(z)$ from large z (bulk) values to the surface. Starting values of $\phi_\pm(z)$ and its derivative in the bulk were determined trivially from Eq. (3) with $V(z) = 0$. The acceptable eigenfunctions for subband j, $\phi_\pm^j(z, k_t)$, are those which satisfy the boundary conditions.

It is interesting to note the formal analogy between Eq. (1) and the Bogoliubov equations which describe quasiparticle dynamics in the Meissner layer of a superconductor.[12] The quasiparticles occupy a quasidiscrete spectrum of states where the transverse kinetic energy dictates the binding condition in a manner similar to the motional binding considered here for a narrow-gap semiconductor.

B. Semiclassical self-consistent potential

The essence of a self-consistent calculation is to solve the Schrödinger equation and Poisson's equation simultaneously. By using the classical approximation in which the electron density is taken as

$$n(z) = k_F^3(z) / 12\pi^2 \ , \tag{4}$$

where k_F is the Fermi wave vector, Ando[13] achieved close agreement with more elaborate self-consistent calculations for narrow-gap semiconductors. The Schrödinger equation was solved in the WKB approximation:

$$\int_0^{z_j} k_z \, d_z = (j + \tfrac{3}{4})\pi \ , \tag{5}$$

where z_j is the classical turning point and k_z is related to the subband energies E_j by the two-band relation, in the same approximation as pertains to Eq. (1),

$$\frac{\hbar^2}{2m^*}(k_z^2 + k_t^2) = [E_j - V(z)] \left[1 + \frac{E_j - V(z)}{E_g}\right] \ , \tag{6}$$

with $m^* = m_l^* = m_t^*$, appropriate for InAs. The semiclassical approximation was also applied by Radantsev *et al.*[5] to InAs, but motional binding solutions were apparently not noticed. Below we use the Ando method to focus on the motional binding regime in the InAs accumulation layers.

III. RESULTS

For a sample in a magnetic field, the frequency, B_f, of Schubnikov–de Haas oscillations is simply proportional to the area of the electronic orbit on an extremal portion of the Fermi surface. The observed "pinning" of B_f was explained in Ref. 1 as due to the near independence of the Fermi "surface" area πk_F^2 on surface-electron density N_s in the motional binding regime. In this section we examine this regime with both a parametrized exponential potential and a semiclassical self-consistent potential.

Figure 1 shows the situation we wish to study. For a given range of bound-state surface-electron density N_s^b, the first-excited state, $j = 1$, will be motionally bound such that its subband exists only for $k_t \geq k_{c1}$. If the Fermi energy, determined from the bulk carrier concentration, n, is larger than the energy corresponding to k_{c1}, the subband is occupied. In the N_s^b range where this motionally bound subband is occupied, the SdH frequency, given by

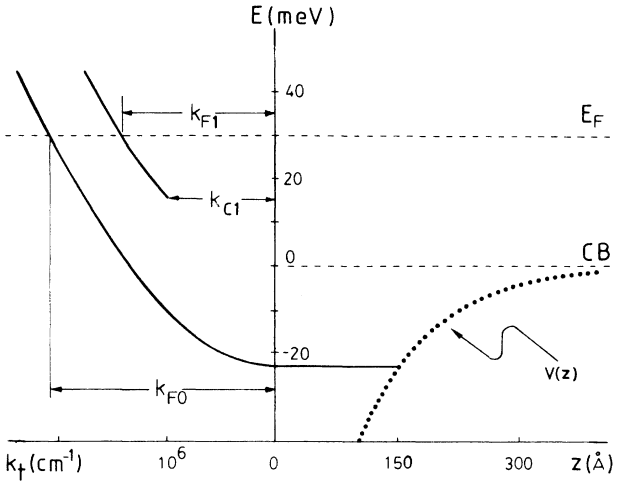

FIG. 1. Exponential potential well and subband dispersion for an n-InAs accumulation layer under motional binding conditions for the first-excited state. The bottom of the conduction band (CB) in the bulk is taken as the zero of energy.

$(c\hbar/2e)k_{F1}^2$ for an isotropic, spin-degenerate system, is not proportional to the subband occupancy, $N_{s1} = (k_{F1}^2 - k_{c1}^2)/2\pi$.

We first use the parametrized exponential potential to analyze the SdH data of Ref. 2. To adjust the parameters of the potential, $-V_0 e^{-z/\lambda}$, we use the experimentally determined intersubband spacings[10] for a degenerate n-InAs sample with $E_F = 30$ meV above the conduction-band edge. With $\lambda = 90$ Å, we find that the first excited state ($j=1$) is occupied and motionally bound for $120 > V_0 < 139$ meV. The subband structure of Fig. 1 corresponds to a voltage in this range ($V_0 = 130$ meV). It is then straightforward to determine the predicted SdH frequency as a function of bound-state electron density, $N_s^b = N_{s0} + N_{s1}$. The result, plotted in Fig. 2, is similar to that found in Ref. 1 with a square-well potential. The motional binding regime is characterized by a nearly flat dependence of B_f on N_s^b with a discontinuity in slope occurring when the subband becomes fully bound ($k_{c1}=0$). The experimental data do not show such a discontinuity, but the range of N_s over which B_f is essentially flat is substantial as the model predicts.

The slope discontinuity is removed in the self-consistent calculation, also shown in Fig. 2. This is due to the nonlinearity introduced by the dependence of the potential $V(z)$ on the electron density N_s which couples k_F and k_c. The arrow in Fig. 2 marks the density at which the subband becomes fully bound ($k_{c1}=0$). Again we see the N_s range of motional binding is well described by the model. The differences in slope and onset N_s value for subband occupancy between the model curve and the experimental curve may be caused by our neglect of the contribution of the charge in the free (unbound) charge density of N_s. The experimental N_s scale includes this contribution.[2] Furthermore, this same dependence of N_s on free charge density causes complications in experimentally determining the zero of the N_s scale.[2,5]

Because the range of N_s over which motional binding occurs for a given subband increases with E_F, it is of interest to examine the frequency B_f of the quantum oscillations in a sample with higher bulk concentration. Figure 3 shows the experimental results of Radantsev *et al.*[5] for the ground-state subband in a sample with $E_F = 156$ meV. To compare our calculation directly to the data, we have replotted the experimental points using the dependence of bound-state density N_s^b on total N_s given in Ref. 5; for the ground state this simply involves an extrapolation of the observed B_f values (outside the motional binding regime) to $N_s = 0$. Our calculation predicts a substantially larger N_{s0} range of motional binding than the data suggest. It may be, however, that the oscillations in the motional binding regime are difficult to observe because B_f becomes independent of gate voltage. The existence of motionally bound carriers over such large N_s ranges means that the contribution of unbound carriers to the surface screening is considerably less important than suggested previously.[2,5]

The independence of B_f on N_s is nicely illustrated when one calculates the Landau-level structure in the motional binding regime. This is easily accomplished by replacing k_t^2 in Eq. (3) with $2n/l^2$, where l is the magnetic length, $l = (\hbar c/eB)^{1/2}$, and n is the Landau index.[14] Figure 4 shows the lowest ten Landau levels for subband

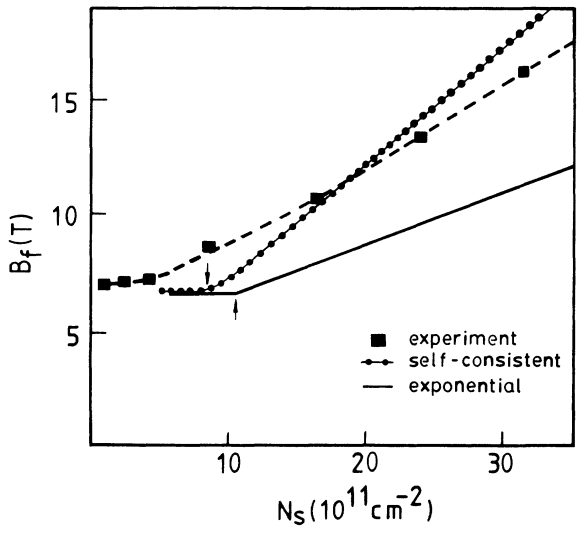

FIG. 2. Comparison of calculated to measured SdH frequency vs carrier density for the motional binding regime of the first-excited subband in an n-InAs accumulation layer ($n = 2\times10^{16}$ cm^{-3}). The experimental data (Ref. 2) is plotted against total, bound and free, gate-voltage-induced carrier density while the calculation is plotted against bound carrier density only. The arrows mark the transition from motional to full binding in the calculations.

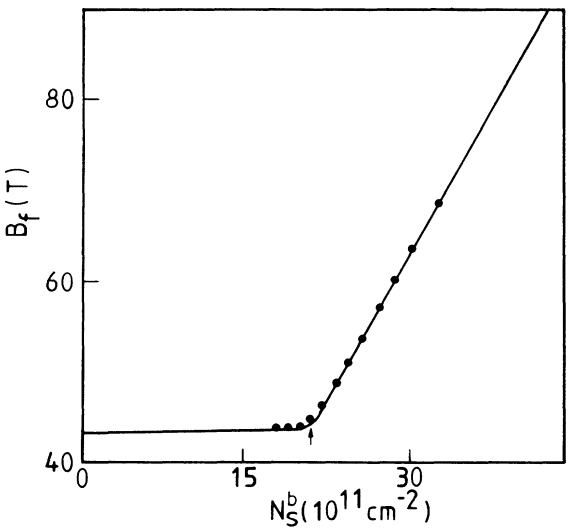

FIG. 3. Quantum oscillation frequency vs bound-state carrier density in a heavily doped n-InAs accumulation layer ($E_F = 156$ meV). The solid curve gives the prediction of the semiclassical self-consistent calculation and the points are taken from the data of Radantsev *et al.* (Ref. 5). The arrow marks the transition from motional to full binding.

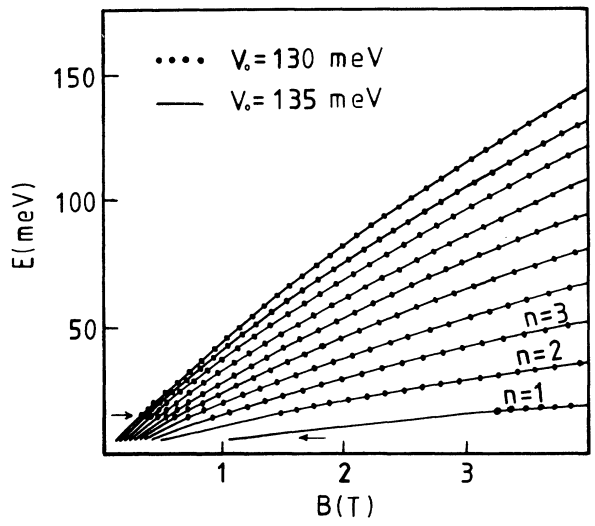

FIG. 4. Allowed energy vs $\hat{z}$-directed magnetic field of the lowest ten Landau levels for a motionally bound subband. The arrows indicate the energy, E_c, at which the Landau levels vanish for each V_0. Below E_c the carriers are no longer bound. The $n=0$ level does not exist in the motional binding regime.

$j=1$ calculated for the exponential potential described above. The values of potential depth in the calculation are both in the range where the subband is motionally bound. Three aspects worth noting are seen in the figure. First, the Landau-level spacing is the same for both V_0 values, reflecting the fact that B_f (which is proportional to the spacing) is independent of V_0, whereas N_s is not in the motional binding regime. Secondly, the Landau-levels vanish at an energy E_c which is the electron energy at $k_t=k_c$. This would not be the case in the absence of motional binding. Finally, the $n=0$ Landau level is nonexistent in the motional binding regime. This is a feature of the two-band model, in which the energy of the $n=0$ level is independent of B and is at the subband bottom E_j. Thus, it vanishes when motional binding occurs. This effect should be observable in systems which are well-described by the two-band model.

IV. CONCLUSIONS

The calculations discussed in this paper indicate that motional binding occurs generally in narrow-gap systems with surface potentials of finite depth, typical of accumulation-layer potentials. In degenerate systems, such as InAs, the motionally bound subbands are occupied over significant ranges of surface-electron density. Therefore, a reexamination of the fully self-consistent calculation introduced by Reisinger[10] (in which motional binding was not noticed) is desirable to clarify the role of free carriers. The large N_s range of motional binding also suggests that the design of quantum-well devices based on motional binding may be possible. For such devices, the transition from bound state to extended state (at $k_t=k_c$) should be abrupt and, at least for InAs, a preliminary study of electron wave functions near k_t indicates that this is the case.[15] It is also of interest in this connection to note the sharp peak in ground-state scattering rate near the population threshold of the first-excited subband observed by Radantsev *et al.*,[5] i.e., near the occupation onset of motionally bound states [$E_F=E(k_c)$]. This would be a particularly interesting regime to explore with intersubband resonance.[10,16]

ACKNOWLEDGMENTS

We are grateful to H. D. Drew for useful discussions. This work was supported by National Science Foundation (NSF) Grant No. RII-86-10676.

[1]R. E. Doezema and H. D. Drew, Phys. Rev. Lett. **57**, 762 (1986).
[2]H. Reisinger, H. Schaber, and R. E. Doezema, Phys. Rev. B **24**, 5690 (1981).
[3]W. Zhao, F. Koch, J. Ziegler, and H. Maier, Phys. Rev. B **31**, 2416 (1985).
[4]V. F. Radantsev, T. I. Deryabina, L. P. Zverev, G. I. Kulaev, and S. S. Khomutova, Zh. Eksp. Teor. Fiz. **88**, 2088 (1985) [Sov. Phys.—JETP **61**, 1234 (1985)].
[5]V. F. Radantsev, T. I. Deryabina, L. P. Zverov, G. I. Kulaev, and S. S. Khomutova, Zh. Eksp. Teor. Fiz. **91**, 1016 (1986) [Sov. Phys.—JETP **64**, 598 (1986)].
[6]G. A. Baraff and J. A. Appelbaum, Phys. Rev. B **5**, 475 (1972).
[7]P. A. Wolff, J. Phys. Chem. Solids **25**, 1057 (1964).
[8]F. J. Ohkawa and Y. Uemura, J. Phys. Soc. Jpn. **37**, 1325 (1974).
[9]F. J. Ohkawa and Y. Uemura, Jpn. J. Appl. Phys. Suppl. **2**, 355 (1974).
[10]H. Reisinger, doctoral dissertation, Technische Universität München, 1983 (unpublished).
[11]Y. Takada, K. Arai, N. Uchimura, and Y. Uemura, J. Phys. Soc. Jpn. **49**, 1851 (1980).
[12]R. E. Doezema, J. N. Huffaker, S. Whitmore, J. Slinkman, and W. E. Lawrence, Phys. Rev. Lett. **53**, 714 (1984).
[13]T. Ando, J. Phys. Soc. Jpn. **54**, 2676 (1985).
[14]See, for example, V. Korenman and H. D. Drew, Phys. Rev. B **35**, 6446 (1987).
[15]J. Slinkman (unpublished).
[16]H. Reisinger and F. Koch, Solid State Commun. **37**, 429 (1981).